Received: 25 February 2023 | Revised: 26 June 2023 | Accepted: 9 October 2023

DOI: 10.1111/pce.14741

ORIGINAL ARTICLE

Plant, Cell & Environment WILEY

Allometries of cell and tissue anatomy and photosynthetic rate across leaves of C_3 and C_4 grasses

Alec S. Baird[1] | Samuel H. Taylor[2] | Sachin Reddi[1] | Jessica Pasquet-Kok[1] | Christine Vuong[1] | Yu Zhang[1] | Teera Watcharamongkol[3,4] | Grace P. John[1,5] | Christine Scoffoni[1,6] | Colin P. Osborne[3] | Lawren Sack[1]

[1]Department of Ecology and Evolutionary Biology, University of California Los Angeles, Los Angeles, California, USA

[2]Lancaster Environment Centre, Lancaster University, Lancaster, UK

[3]Department of Animal and Plant Sciences, University of Sheffield, Sheffield, UK

[4]Faculty of Science and Technology, Kanchanaburi Rajabhat University, Kanchanaburi, Thailand

[5]Department of Biology, University of Florida, Gainesville, Florida, USA

[6]Department of Biological Sciences, California State University Los Angeles, Los Angeles, California, USA

Correspondence
Alec S. Baird, Department of Ecology and Evolutionary Biology, University of California Los Angeles, Los Angeles, California, USA.
Email: alecsbaird@gmail.com

Funding information
US National Science Foundation, Grant/Award Numbers: 1457279, 1951244, 2017949, 1943583; Natural Environment Research Council, Grant/Award Numbers: NE/DO13062/1, NE/T000759/1

Abstract

Allometric relationships among the dimensions of leaves and their cells hold across diverse eudicotyledons, but have remained untested in the leaves of grasses. We hypothesised that geometric (proportional) allometries of cell sizes across tissues and of leaf dimensions would arise due to the coordination of cell development and that of cell functions such as water, nutrient and energy transport, and that cell sizes across tissues would be associated with light-saturated photosynthetic rate. We tested predictions across 27 globally distributed C_3 and C_4 grass species grown in a common garden. We found positive relationships among average cell sizes within and across tissues, and of cell sizes with leaf dimensions. Grass leaf anatomical allometries were similar to those of eudicots, with exceptions consistent with the fewer cell layers and narrower form of grass leaves, and the specialised roles of epidermis and bundle sheath in storage and leaf movement. Across species, mean cell sizes in each tissue were associated with light-saturated photosynthetic rate per leaf mass, supporting the functional coordination of cell sizes. These findings highlight the generality of evolutionary allometries within the grass lineage and their interlinkage with coordinated development and function.

KEYWORDS

carbon concentrating mechanism, development, functional traits, growth, morphology, scaling

1 | INTRODUCTION

Relationships among the quantitative properties of cells, organs and organisms, that is, allometries, provide insights into evolution, development and function (Baird et al., 2021; Huxley, 1932; John et al., 2013; Meinzer et al., 2003; Niklas, 1994; Sack et al., 2012; Smith & Sperry, 2014; Sperry et al., 2005; Zhong et al., 2020). Across diverse eudicotyledons, cell sizes in the leaf epidermis and mesophyll are positively correlated, but independent from xylem cell sizes; further, cell dimensions increase with leaf thickness (John et al., 2013). Such allometries would arise from coordinated development during leaf expansion, and may be reinforced by selection as coordination in cell sizes leads to efficient transport of water, nutrients and sugars between cells of different types (Cadart & Heald, 2022). Further, allometric analyses of cell properties provide important insights into physiological functions, including rates of

exchange of carbon and water, and environmental stress tolerance (Brodribb et al., 2013; Meinzer et al., 2003; Nobel, 2020; Olson et al., 2018; Smith & Sperry, 2014; Sperry et al., 2005; Zhong et al., 2020).

Leaf anatomical allometries have not been tested for grasses, a family (Poaceae) of 12,000 species diverse in morphology (Supporting Information: Table S1), that dominates 43% of the terrestrial surface, and accounts for the majority of crop production (Beer et al., 2010; McSteen & Kellogg, 2022). The optimisation of grass anatomy is part of Grand Challenge efforts to improve the physiology of stress tolerance and productivity, including the engineering of novel C_4 crops from C_3 precursors (Eckardt et al., 2023; Ermakova et al., 2020; Lowry et al., 2019). Grasses differ from typical eudicotyledons in leaf development and form. Grass leaves arise from an intercalary meristem, in which cells file through distinct zones of division, expansion and differentiation at the leaf base (Table 1; Figure 1; Evert, 2006; Fournier et al., 2005; Skinner & Nelson, 1994) resulting in linearised forms with parallel longitudinal veins

TABLE 1 Glossary of terminology related to allometry, leaf anatomy and grass development.

Term	Definition
Allometry	Study of size related properties, that is dimensions, mass, and/or metabolic processes and consequences for biological function (Huxley, 1932; Niklas, 1994).
Bulliform cell	Specialised enlarged upper epidermal cells that regulate leaf rolling and unrolling via changes in cell turgor (Ellis, 1976; Evert, 2006).
C_4 photosynthesis	Photosynthesis that occurs through compartmentalising and concentrating CO_2 at sites of carbon reduction within bundle sheath, leading to elevated rates of carbon accumulation and minimised photorespiratory losses (Christin et al., 2013; Dengler et al., 1985; Sage, 2004).
Cell size	In this study, the cross-sectional area of the specified cell type.
Culm height	The height of the central grass shoot, typically quantified after flowering, and preceded by shoot elongation (Clayton et al., 2006; Evert, 2006).
Epidermal cell	Cells that form the outer layer of the plant, including the upper and lower surface of leaves, regulating gas exchange and providing protection of internal cells (Evert, 2006).
Furrow	The intercostal zone between vascular bundles that is often much thinner than the leaf section where vascular bundles and mesophyll occur (Ellis, 1976, e.g., Supporting Information: Figure S3d).
Geometric scaling	Proportional changes in dimensional size across species, individuals or organs; indicated by $b = 1$ (i.e., isometry) for relationships among dimensions of the same scale, that is, for lengths with lengths or areas with area, and $b = 0.5$ for relationships of areas with lengths (Huxley, 1932; John et al., 2013; Niklas, 1994).
Intercalary meristem	The growing region at the base of grass leaves, where cells divide, expand and differentiate; surrounded by the grass sheath (Evert, 2006; Fournier et al., 2005; Skinner & Nelson, 1994).
Kranz anatomy	Specialised conformation of leaf cells and tissues, with mesophyll cells arranged closely to parenchymatous vein sheath, facilitating CO_2 concentration from mesophyll to bundle sheath, and CO_2 assimilation in vein sheath (Christin et al., 2013; Dengler et al., 1985; Sage, 2004).
Mesophyll cell	Non-vein cells that contain chloroplasts and generate sugars via photosynthesis (Evert, 2006).
Mestome sheath cell	Inner layer of thick-walled cells that surround vascular bundles, interior to the bundle sheath in most grasses, and is the only sheath in some C_4 grasses, and the only location for carbon reduction; hypothesised to function for regulating water, sugar and hormonal transport in C_3 and C_4 grasses with both sheaths. Arises from procambium (Dengler et al., 1985; Evert, 2006).
Parenchymatous bundle sheath cell	Outer layer of thin-walled parenchymatous cells that surrounds vascular bundles and functions for water and nutrient storage, and regulating water, sugar and hormonal transport; in C_4 plants, location of carbon reduction (Dengler et al., 1985; Evert, 2006; Griffiths et al., 2013).
Plasmodesmata	Channels connecting plasma membranes of adjacent cells that function for symplastic transport, that is exchange of cytoplasmic materials, including proteins and sugars (Danila et al., 2016; Evert, 2006).
Precursor cell	Undifferentiated but often identifiable cells distinct in properties that indicate their mature cell type, for example, procambium (Evert, 2006).
Procambium	Precursor cells to vascular cell types, that is, xylem, phloem and mestome cells, during leaf development, distinct in cytoplasm density, degree of vacuolation and cell elongation (Dengler et al., 1985; Evert, 2006; Nelson & Dengler, 1997).
Type I xylem cell	Enlarged xylem conduit present in major vein orders; much larger but less numerous than type II xylem. Arises from procambium (Baird et al., 2021; Fournier et al., 2005; Nelson & Dengler, 1997).
Type II xylem cell	Smaller xylem conduit present in all vein orders; much smaller but more numerous than type I. Arises from procambium (Baird et al., 2021; Evert, 2006; Nelson & Dengler, 1997).

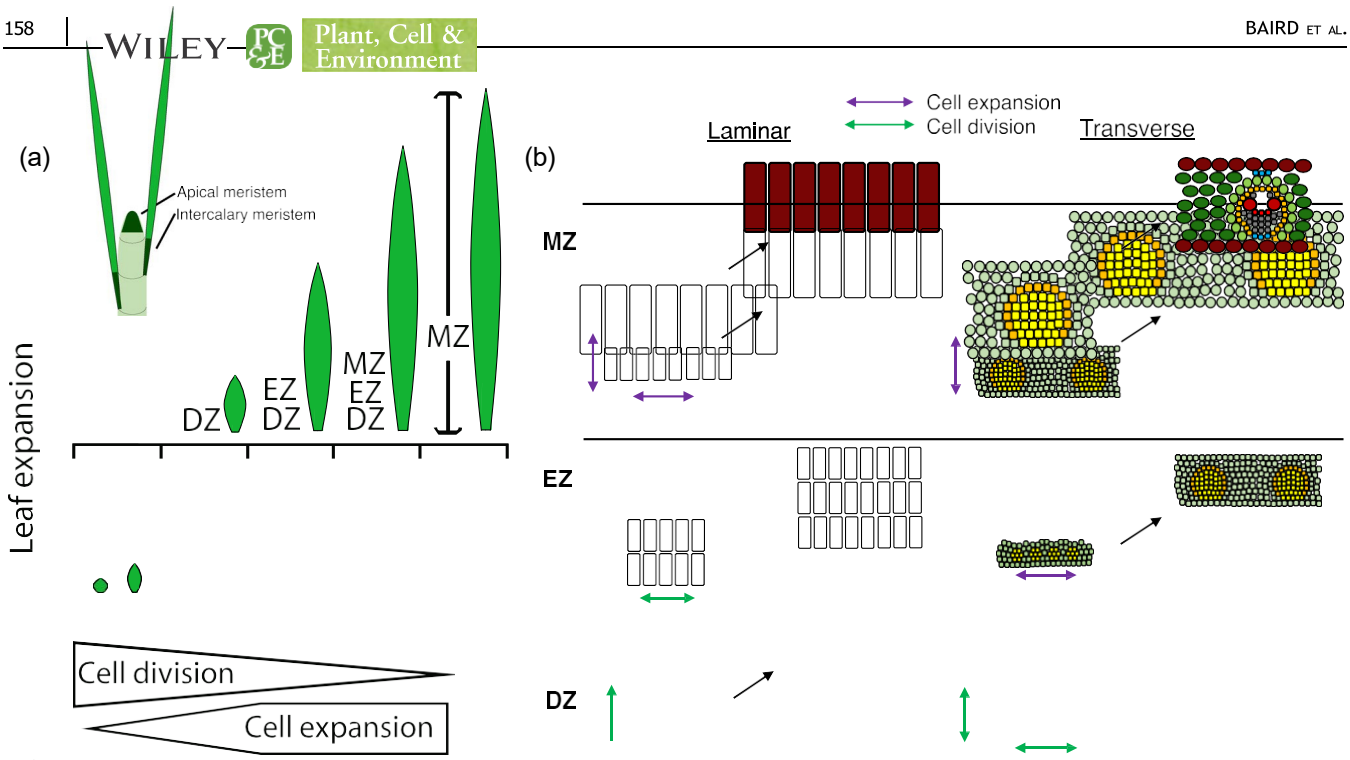

FIGURE 1 Grass leaf development. (a) In grasses, leaf expansion is restricted to distinct developmental zones driven by the generation of the leaf primordium via the apical meristem. Although growth initially begins via the apical meristem, leaf growth becomes restricted to the intercalary meristem at the base of the growing leaf in which cells proliferate in the division zone (DZ), expand laterally and longitudinally in the expansion zone (EZ), and complete their differentiation in the maturation zone (MZ). Thus, growth occurs as cells continuously proliferate in the DZ and then expand in the EZ. (b) Laminar, or projected viewpoint, and transverse visualisations of the different growing zones of a typical C_3 grass, with epidermal cells in the laminar column, and all cell types depicted in the transverse column, with procambium cells shown in orange and yellow (mestome cells shown in orange) and nonprocambium cells shown in light green. Bundle sheath precursors are the cells surrounding the orange mestome sheath cells. The intercalary meristem is typically covered by the grass sheath, and thus protected, but this was omitted from panel (a) so as to illustrate the location of the intercalary meristem with respect to the shoot apical meristem. Panel (a) was originally published in Baird et al., 2021 and modified to include a visualisation of the two grass shoot meristems for this study, and panel (b) was created based on findings from Baird et al. (2021), Dengler et al. (1985), Evert (2006), Fournier et al. (2005), Granier and Tardieu (2009), Skinner and Nelson (1994), Volkenburgh (1999).

connected by transverse veins (Ellis, 1976; Evert, 2006). Like eudicots, grasses possess a parenchymatous bundle sheath surrounding all veins, derived from dividing lamina cells. Yet, grass leaves typically also possess a mestome sheath interior to the vein bundle sheath, which is derived from procambium precursors, like the xylem and phloem (Dengler et al., 1985; Evert, 2006). Further, 41% of grasses have C_4 photosynthesis, and these possess specialised "Kranz" anatomy, including higher vein length per area, enlarged sheath cells, and much more extensive plasmodesmata connecting mesophyll with sheath cells, relative to C_3 grasses (Christin et al., 2013; Danila et al., 2016; Dengler et al., 1985; Sage, 2004), all of which contribute to their C_4 syndrome that confers higher rates of CO_2 uptake and tolerance to aridity and extreme temperatures (Sage, 2004; Watcharamongkol et al., 2018).

Across species, we hypothesised a framework of inter-related anatomical allometries ("scaling relationships") of the form

$$y = ax^b \text{ or } \log y = \log a + b \log x, \quad (1)$$

where y and x are dimensions, and a and b the allometric intercept and slope (Table 2). First, we hypothesised *allometries among cell dimensions* due to proportional development, and, additionally, due to cell size coordination for integrated function (Table 2; Brodribb et al., 2013; Cadart & Heald, 2022; Granier & Tardieu, 1998; Volkenburgh, 1999; see Supporting Information: Appendix, "Relationship of leaf developmental and evolutionary allometries, and insights into development and function"). Second, we hypothesised that *leaf dimensions would be related to those of their constituent cells* (Table 2; John et al., 2013). Third, we hypothesised that *xylem cell areas would increase with leaf size and plant height*, such that xylem water transport capacity would at least in part compensate for the longer transport pathlengths in longer leaves of taller grasses (Table 2; Baird et al., 2021; Olson et al., 2018). Fourth, we hypothesised that grasses would show *similar leaf anatomical scaling as eudicots*, with exceptions arising from their different leaf morphology (Table 2, Supporting Information: Appendix). We expected that grasses would differ from eudicots in some leaf allometries, given their fewer cell layers, highly elongated shape and specialised roles of the epidermis and bundle sheath, including high shrinkage and expansion capacity allowing for leaf movements (including rolling), and/or water storage enabling buffering of low-resource availability. We thus expected grasses to differ from eudicots in allometries for cell cross-sectional areas of epidermis and bundle sheath versus overall leaf dimensions. Lastly, we hypothesised that across grass species, light-saturated photosynthetic rate per leaf mass

TABLE 2 Framework of hypotheses tested in this study, rationale for hypotheses, traits measured and if the hypothesis was supported (see Table 1 for definitions of terminology).

Hypothesis	Rationale	Relationships measured (y vs. x)	Hypothesis supported
1. Positive allometries among cell cross-sectional areas	Cells may have proportional development, reinforced by integrated function by cell size coordination.	The cross-sectional areas of: Epidermises versus mesophyll; Epidermises versus parenchymatous bundle sheath; Epidermises versus mestome sheath; Epidermises versus type I xylem; Epidermises versus type II xylem; Mesophyll versus parenchymatous bundle sheath; Mesophyll versus mestome sheath; Mesophyll versus type I xylem; Mesophyll versus type II xylem; Parenchymatous bundle sheath versus mestome sheath; Parenchymatous bundle sheath versus type I xylem; Parenchymatous bundle sheath versus type II xylem; Mestome sheath versus type I xylem; Mestome sheath versus type II xylem; Type I versus type II xylem.	Yes
2. Positive allometries of leaf dimensions and the cell cross-sectional areas of constituent cells	Cells are building blocks of dimensions of the whole organ, particularly that of leaf thickness and width.	Leaf thickness and leaf width versus the cross-sectional areas of epidermises; Leaf thickness and leaf width versus the cross-sectional area of mesophyll; Leaf thickness and leaf width versus the cross-sectional area of parenchymatous bundle sheath; Leaf thickness and leaf width versus the cross-sectional area of mestome sheath; Leaf thickness and leaf width versus the cross-sectional area of type I xylem; Leaf thickness and leaf width versus the cross-sectional area of type II xylem.	Yes
3. Positive allometries of leaf size and plant height with cross-sectional areas of procambium derived cell types	Longer leaves and taller plants would require larger xylem for optimal hydraulic design/delivery. Mestome sheath cells may also show scaling, from being derived from the procambium.	Leaf length, leaf area and culm height versus the cross-sectional area of mestome sheath; Leaf length, leaf area and culm height versus the cross-sectional area of type I xylem; Leaf length, leaf area and culm height versus the cross-sectional area of type II xylem.	Yes
4. Grasses would show similar leaf anatomical scaling as eudicots, with exceptions arising from their different leaf morphology	In grasses, the fewer cell layers, highly elongated leaf blade and specialised roles of bundle sheath and bulliform epidermal cells drives different allometries.	Leaf length, leaf area and culm height versus the cross-sectional areas of epidermises; Leaf length, leaf area and culm height versus the cross-sectional area of mesophyll; Leaf length, leaf area and culm height versus the cross-sectional area of parenchymatous bundle sheath.	Yes
5. Positive allometries of and light-saturated photosynthetic rate per leaf mass (A_{mass}) and cell cross-sectional areas	Allometries of cell dimensions in hypothesis one would arise from the coordination of cell function	A_{mass} versus the cross-sectional areas of epidermises; A_{mass} versus the cross-sectional area of mesophyll;	Yes

(Continues)

TABLE 2 (Continued)

Hypothesis	Rationale	Relationships measured (y vs. x)	Hypothesis supported
	(transport, metabolism and/or photosynthesis).	A_{mass} versus the cross-sectional area of parenchymatous bundle sheath; A_{mass} versus the cross-sectional area of mestome sheath; A_{mass} versus the cross-sectional area of type I xylem; A_{mass} versus the cross-sectional area of type II xylem.	

(A_{mass}) would scale positively with cell sizes in multiple tissues due to the integrated impact of cell size on leaf structure and function (Table 2). A_{mass} is equivalent to light-saturated photosynthetic rate per leaf area (A_{area})/leaf mass per area (LMA) (Sack et al., 2013). Given that leaves with large cells would tend to be thicker (John et al., 2017), we hypothesised they would have higher A_{area}, as previously found in studies of grasses and eudicotyledonous species (Charles-Edwards et al., 1974; Garnier et al., 1999; Koike, 1988; Wilson & Cooper, 1967), and that they would be wider, with lower major vein length per area (Baird et al., 2021), contributing to a lower *LMA* (John et al., 2017). Further, larger xylem conduits drive higher hydraulic supply which would enable higher A_{area} and would also be reflected in a high A_{mass}.A parallel coordination of A_{mass} with cell sizes in multiple tissues, including photosynthetic mesophyll and xylem transport tissue, would further support our first hypothesis of functional coordination of cell sizes throughout the leaf for metabolism and transport.

For the majority of relationships among cell and leaf dimensions, we expected that proportional development would result in *geometric allometries*, which would be reinforced by selection for coordinated and integrated function. Thus, areas (A) would scale together isometrically as $A \propto A^1$ and with lengths (L) as $L \propto A^{1/2}$ (Table 1; Supporting Information: Appendix; Baird et al., 2021; John et al., 2013; Niklas, 1994; Sack et al., 2012). We expected divergences from geometric scaling, that is, decoupling of proportional development, for certain functionally specialised tissues (Table 3). Thus, relative to other cell types, we expected disproportional increases in cell size for the upper epidermis, reflecting a greater investment in supporting functions including large specialised bulliform cells that provide water storage and enable leaf rolling (Ellis, 1976; Evert, 2006). Further, we expected divergence from geometric scaling for allometries among xylem cell types that would be coordinated for optimal hydraulic design; for the major and minor vein systems to maintain matched transport efficiency across leaves of different size, the size of type I xylem conduits (which occur only in major veins) would increase disproportionately relative to type II xylem (which occur in both major and minor veins) to compensate for the declining density of major veins that are spaced out further in larger leaves (Baird et al., 2021). We expected leaf dimensions to increase disproportionately with cell cross-sectional areas, as dimensions also depend on the additional role of cell number, which in larger leaves increases disproportionately relative to cell areas (Gázquez & Beemster, 2017; John et al., 2017). We expected leaf length and culm height would increase disproportionately relative to vein xylem cell sizes; increases in xylem cell size that would mitigate of impacts of increasing path length need not be proportionate, because hydraulic conductance through xylem increases as the radius to the fourth power (Sack & Scoffoni, 2013). Finally, we expected that C_3 and C_4 grasses would differ in allometries, with more generalised relationships across all cell types across C_3 species, because specialised C_4 cell functions associated with Kranz anatomy and carbon concentrating mechanism, including higher densities of plasmodesmata (Danila et al., 2016), may disrupt cell size-function relationships. We expected that for C_4 species, selection for enlarged sheath cells (Christin et al., 2013) would decouple the cell cross-sectional areas of bundle and mestome sheaths, mesophyll and xylem.

To test this framework of hypothesised general relationships, we used a common garden, glasshouse experiment to measure leaf anatomy and photosynthetic rate in a phylogenetically structured sample of 27 grass species.

2 | MATERIALS AND METHODS

2.1 | Study species and sampling

We selected 27 grass species to represent high functional and phylogenetic diversity, encompassing 11 C_4 origins (16 C_4 species; 11 C_3 species), and including terrestrial and aquatic species and important crops (Figure 2; Supporting Information: Figures S1–S3; Supporting Information: Table S1). Plants were grown in a common garden to minimise environmentally-driven plasticity. The individuals sampled for anatomical measurements in this study (see "Anatomical sample preparation and measurements") were the same individuals and leaves sampled for leaf size and venation traits in a previous publication (Baird et al., 2021).

Seeds were acquired from seed banks and commercial sources (Supporting Information: Table S1), and before germination were surface-sterilised with 10% NaClO and 0.1% Triton X-100 detergent, rinsed with sterile water, and sown on plates of 0.8% agar sealed with Micropore surgical tape (3M). Seeds were germinated in chambers maintained at 26°C, under moderate intensity cool white fluorescent lighting with a 12-h photoperiod. When roots ranged from 2 to 3 cm long, seedlings were transplanted to 3.6 L pots with potting soil

TABLE 3 Explanations for allometries of grass leaf cells based on geometric scaling.

Allometry	y versus x relationship	Allometric slope b observed	Explanation for expected slope b
1. Scaling of cell areas within and across tissues§	Mesophyll versus upper epidermis	<1	Disproportionately large increase of upper epidermis required for storage and support relative to increase of mesophyll cell size.
	Mesophyll versus bundle sheath	<1	Disproportionately large increase of bundle sheath required for storage and support relative to mesophyll cell size.
	Type II xylem versus type I xylem	<1	For the major and minor vein systems to maintain matched transport efficiency across leaves of different size, type I xylem conduit sizes must increase disproportionately relative to type II xylem to compensate for the declining vein density of major veins.
	Type II xylem versus mestome sheath	>1	Shorter development time for mestome sheath cells than type I xylem would result in diminishing scaling as mestome sheath cells form relatively late in the sequence of leaf and vein development.
	Mestome sheath versus bundle sheath	<1	Longer development time for bundle sheath than mestome sheath enables departed scaling, as mestome sheath cells forms relatively late in the sequence of leaf and vein development, reinforced by functional coordination of sheath sizes, to match radial transport capacity through both sheaths.
	Type II xylem versus bundle sheath	<1	Longer development time for bundle sheath than type II xylem enables departed scaling, as type II xylem forms relatively late in the sequence of leaf and vein development, reinforced by functional coordination, to match radial transport capacity out of the xylem with axial (longitudinal) transport capacity.
	Mestome sheath versus upper epidermis	>1	Longer development time for mesophyll than mestome sheath enables disproportionate scaling, as mestome sheath forms relatively late in the sequence of leaf and vein development, reinforced by functional coordination of sheath and epidermal cell sizes, to match transport capacity with demand.
	Mestome sheath versus lower epidermis	>1	"
2. Scaling of leaf and plant dimensions with nonxylem cell areas	Leaf width versus mesophyll	>0.5	Cell size in a given tissue is one of a series of contributors to whole leaf dimensions, including also numbers of cells or cell layers, and cells of other tissues.
	Leaf width versus bundle sheath	>0.5	"
	Culm height versus bundle sheath	>0.5	Less than proportionate increases of bundle sheath cell size relative to culm height (and thus disproportionate increases in culm height relative to bundle sheath) would be sufficient to limit path length constraints to flow, as the bulk of path length is through xylem.
3. Scaling of leaf and plant dimensions with xylem cell areas	Leaf length versus type I xylem	>0.5	Less than proportionate increases of xylem cell size relative to organ length or plant size (and thus disproportionate increases in organ length and plant size relative to xylem) would be sufficient to limit path length constraints to flow, as flow rate through xylem increases as the radius to the fourth power, and thus would not need to increase proportionally.

(Continues)

TABLE 3 (Continued)

Allometry	y versus x relationship	Allometric slope b observed	Explanation for expected slope b
	Leaf length versus type II xylem	>0.5	"
	Culm height versus type I xylem	>0.5	"
	Culm height versus type II xylem	>0.5	"
Eudicot scaling[a] 4. Similar scaling of grasses and eudicots, except for those of mesophyll versus upper epidermis	Mesophyll versus upper epidermis	<1	Scaling would be lower in grasses due to disproportionately large increase of upper epidermis required for mechanical support, storage and leaf movements relative to increase of mesophyll cell size.

Note: Expectations for *b* may depart from geometric scaling when (1) developmental processes for cells differ in the timing or rates of growth, especially when tissues form relatively late in the sequence of leaf development; thus, we expected disproportionate scaling of cell sizes in nonprocambium derived tissue with mestome sheath cells, and of type II xylem with bundle sheath in C_3 species, and of type II xylem with type I xylem across all species, (2) due to selection on function of a specific tissue, as would apply to the scaling of mesophyll with the upper epidermis or bundle sheath, which would increase in size disproportionately to mesophyll, leading to greater storage and support in upper epidermis and bundle sheath and departure from geometric scaling for mesophyll versus upper epidermis, and for mesophyll versus bundle sheath, (3) due to constraints imposed by coordinated optimal vascular design, as would apply to the disproportionate scaling of type II xylem with type I xylem, as type II xylem occur only in major veins, and thus need to increase in size to compensate for the declining density of major veins and (4) for relations of cell areas and whole leaf dimensions, as different cell types differ in number, which would impact the contribution of one cell type scaling with a whole leaf dimension.

[a]Our analysis of data from John et al. (2013).

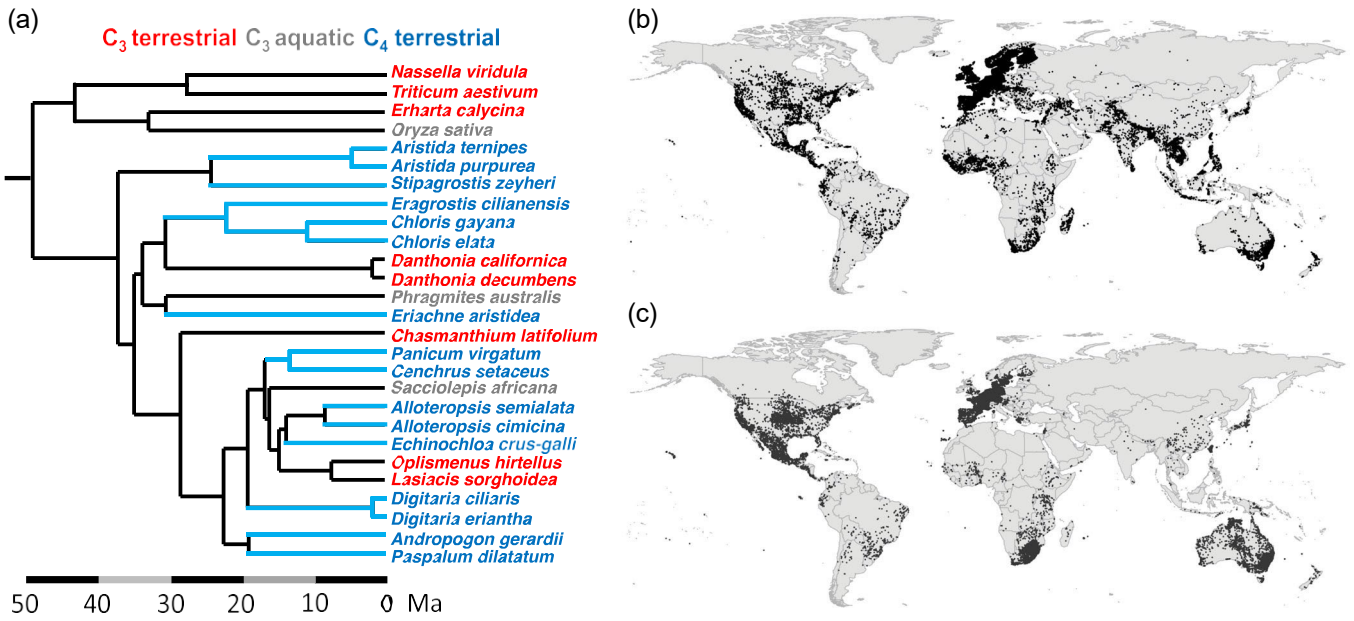

FIGURE 2 Phylogenetic tree used to account for the influence of species relatedness on scaling relationships, and species distribution maps. (a) All 27 grass species included in the study. Distributions of (b) 11 C_3 grass species and (c) 16 C_4 grass species. Blue branches in (a) indicate a C_4 evolution, including 11 total independent evolutions. [Color figure can be viewed at wileyonlinelibrary.com]

(1:1:1.5:1.5:3 of coarse vermiculite: perlite: washed plater sand: sandy loam: peat moss). Plants were grown in a common garden at the UCLA Plant Growth Center (minimum, mean and maximum daily values for temperature: 20.1°C, 23.4°C and 34.0°C; for relative humidity: 28%, 50% and 65%; and mean and maximum photosynthetically active radiation during daylight period: 107 and 1988 μmol photons m^{-2} s^{-1}; HOBO Micro Station with Smart Sensors; Onset). To reduce the impacts of variation in light and temperature on plant growth and traits, plants were arranged in six randomised blocks across three benches, with one individual per species per block (n = 6 except *Alloteropsis semialata*, n = 4) and two blocks per bench. Plants were irrigated daily with water containing fertiliser

(200–250 ppm of 20:20:20 N:P:K; Scotts Peters Professional water soluble fertiliser; Everris International B.V.). We grew all 27 species in potting soil, including the three species classified as aquatic (*Oryza sativa*, *Phragmites australis*, *Sacciolepis africana*), to maximise similarities in growth conditions across species; as in previous studies these aquatic grasses grew to maturity under nonaquatic conditions (Clevering, 1999; Kato & Okami, 2010). All species were grown until flowering to verify species identities.

2.2 | Anatomical sample preparation and measurements

For three individuals per species that possessed many mature leaves, one leaf was fixed and stored, and 1 μm thick transverse cross sections were prepared, stained, and imaged by light microscopy (Fletcher et al., 2018; John et al., 2013; Nobel, 1976; Nobel et al., 1975) (Leica Leitz DMRB; Leica Microsystems with SPOT Imaging Solution camera; Diagnostic Instruments, Sterling Heights). Leaves were fixed and stored in FAA solution (37% formaldehyde-glacial acidic acid-95% ethanol in deionized water). Central rectangular samples were cut from each leaf halfway along the length of the blade and gradually infiltrated under vacuum with low-viscosity acrylic resin (L. R. White; London Resin Co.). Infiltrated samples were set in resin in gelatin capsules to dry at 55°C overnight. Transverse cross sections of 1 μm thickness and of varying width (species dependent) were prepared using glass knives (LKB 7800 KnifeMaker; LKB Produkter; Bromma, Sweden) in a rotary microtome (Leica Ultracut E, Reichert-Jung California), placed on slides and stained with 0.01% toluidine blue in 1% sodium borate (w/v). Slides were then imaged at 5×, 20×, and 40× objective using a light microscope (Leica Lietz DMRB; Leica Microsystems) and camera with imaging software (SPOT Imaging Solution; Diagnostic Instruments, Sterling Heights).

We quantified leaf thickness and cell cross-sectional areas of the mesophyll, upper and lower epidermis, parenchymatous bundle and mestome sheaths and xylem using the programme ImageJ (Fletcher et al., 2018; John et al., 2013; Nobel, 1976; Nobel et al., 1975) (ImageJ version 1.42q; National Institutes of Health). Cell cross-sectional area was used as an index of cell size (Nobel, 2020), which would reflect cell volumes in the case of mesophyll cells, which are symmetrical in shape, but not for epidermal, vascular sheath and xylem cells, which differ in shape between transverse and paradermal planes (Nobel, 1976; Nobel et al., 1975). Measurements of cells of the mesophyll and the lower and upper epidermis were replicated three times for each cross section. In the middle of the left, center and right thirds of the cross section, mesophyll cells were selected for determination of cell area and, given their irregular shapes, were traced. We measured leaf thickness three times at the left, center and right thirds of the cross section that excluded leaf furrows (Table 1; Ellis, 1976). Epidermal cells were similarly selected, but their areas were determined as the area of an ellipse, area = $\pi \times a \times b$, where a and b are the radii of the major and minor axes, that is, the lengths and widths of the cells. Dimensions of parenchymatous bundle and mestome sheath cells and xylem conduits were quantified for each specific vein order, and their areas determined as for epidermal cells. Cells were measured for vein xylem and parenchymatous bundle and mestome sheaths in the major veins, that is, the 1° "midvein" and 2° "large" veins, and in the minor veins, that is, the 3° "intermediate" veins, and, for the species that possessed them, the 4° "small" veins; these 4° "small" veins occur in one C_4 clade (the NADP-ME of Panicodeae), represented by seven species in this study, for which the mestome sheath functions for carbon reduction and is the only vein sheath, excluding *A. semialata* which possesses 4° veins, and has both sheaths (Dengler et al., 1985). To reduce biases in calculating average xylem cell sizes, we differentiated two metaxylem conduit types within the major veins, which is consistent with previous studies noting that these conduit types are clearly developmentally and functionally distinct (Dannenhoffer et al., 1990; Russell & Evert, 1985). The major veins contain large "type I xylem" conduits, and both major and minor veins contain the distinctively smaller "type II xylem" conduits (Baird et al., 2021). For each vein order, we selected one small, one medium and one large parenchymatous bundle sheath cell (same for mestome sheath cells), and determined their average area, and we quantified all xylem cell areas within each vein order, and averaged these for type I and for type II xylem. We also calculated average parenchymatous bundle and mestome sheath and type I and II xylem cell areas across all vein orders. We did not quantify second-order vein or sheath traits for the species *Lasiacis sorghoidea*, as we lacked high magnification images that included their very widely spaced second-order veins. We did not quantify phloem cell dimensions due to the inability to competently distinguish sieve cells from parenchyma in the images.

We also utilised published values for maximum leaf length and width, and leaf area as their product, and published values for culm height data as a measure of plant height, to test relationships with leaf and plant morphology with cross-sectional cell areas (Baird et al., 2021; Clayton et al., 2006). The product of maximum length and width overestimates leaf area for grasses; however no standard correction value exists for grasses (Kemp, 1960; Shi et al., 2019; Stickler et al., 1961). Considering the diverse set of leaf shapes included in our experiment, and noting that a correction factor is unlikely to impact differences on the log scales used for the correlation coefficients, scaling exponents and their statistical significance, we did not apply a correction factor and our estimates of leaf area should be taken as approximate. We utilised published data for major vein length per leaf area (VLA_{major}; Baird et al., 2021) to test relationships of cell cross-sectional areas with VLA_{major}.

2.3 | Quantification of leaf gas exchange

Leaf gas exchange data for the eight C_3 terrestrial grasses was previously published (Baird et al., 2021). For all 27 grass species, including the eight C_3 terrestrial grasses, we measured light-saturated rates of gas exchange from 17 February to 28 June 2010, between

0900 and 1500 each day, for a mature leaf on each plant for six plants per species. We measured steady state gas exchange (<2% change over 6 min) using a LI-6400XT portable photosynthesis system (LI-COR, Lincoln). The leaf chamber was maintained at 25°C, with reference CO_2 400 ppm, and PPFD 2000 μmol m^{-2} s^{-1}, which was assumed to be saturating irradiance for these species (Taylor et al., 2010). The ranges of relative humidity and vapour pressure deficit (VPD) were respectively 60%–80% and 0.80–1.6 kPa (overall mean 1.1 kPa). Measurements were made for 1–2 leaves from each of six plants (except from 5, 4 and 7 plants for *A. purpurea*, *A. semialata* and *P. australis* respectively, and for 3 leaves from each of two plants for *L. sorghoidea*); overall, 5–9 leaves (mean of 6) were measured per species. Leaf-area normalised values were determined for net photosynthetic rate per leaf area (A_{area}). Leaves were harvested, scanned for leaf area (Canon Scan Lide 90, Canon USA, Lake Success), dried at 70°C for at least 48 h and weighed to determine the leaf dry mass per unit area (LMA). Net CO_2 assimilation rate per unit leaf dry mass (A_{mass}) values were determined as A_{area}/LMA.

2.4 | Data analysis

Before testing cross-species relationships, we evaluated whether species differed meaningfully in mean trait values, using a non-phylogenetic analysis of variance (ANOVA) on all traits, and tested for the influence of species identity, such that residual error was associated with replicate individuals of a species, enabling estimation of the percent of variation in each trait arising across species relative to that arising among individuals of the same species (Supporting Information: Table S2).

Using a published phylogeny, we tested trait-trait relationships across all species and within particular groups: C_3 grasses; C_4 grasses; C_3 terrestrial, that is, removing the C_3 aquatic species (which were in several cases outliers); and C_4 + C_3 terrestrial (Figure 2; Baird et al., 2021). For comprehensiveness, we tested relationships among cell sizes for the seven tissue types (i.e., 21 pairwise combinations). For vein type I and II xylem, and parenchymatous bundle and mestome sheath cells, relationships were tested within each vein order (six pairwise combinations each for 1° and 2° veins; three for 3° veins, lacking type I xylem; and 1 for 4° veins, lacking type I xylem and parenchymatous bundle sheath = 16 combinations). Analyses were performed using the R Language and Environment, modifying published code with phylogenetic functions (Baird et al., 2021). We fitted lines to log-transformed data, the typical approach in allometric analyses (Baird et al., 2021; Niklas, 1994; Poorter & Sack, 2012; Warton et al., 2006). We used the phytools package (Revell, 2012) to fit phylogenetic reduced major axes regressions (PRMA) for the majority of scaling relationships. Because only seven species had fourth order veins, we used non-phylogenetic standard major axis (SMA; a synonym of reduced major axis, i.e., RMA; Warton et al., 2006) regression to evaluate scaling of fourth order vein cell area traits with other cell areas (Baird et al., 2021; Niklas, 1994; Poorter & Sack, 2012; Warton et al., 2006).

Typically, allometric relationships arise as two-parameter power laws with zero intercepts when considered with untransformed data (Equation 1). As is typical of allometric studies, we considered a slope to be consistent with geometric scaling when its 95% confidence interval included the test value (Baird et al., 2021; Poorter & Sack, 2012). We tested for differences in trait means between C_3 and C_4 species using a phylogenetically corrected analysis of variance, both parametric and nonparametric (Garland et al., 1993; Revell, 2012).

For several relationships in our study, data were inconsistent with a power-law, because they had a clear nonzero intercept. In these cases, linear relationships fitted well:

$$y = bx + a, \tag{2}$$

where y and x are dimensions, and a and b are the intercept and slope. When y and x have the same dimensionality (i.e., two areas, or two lengths), a positive linear relationship would support geometric (proportional) scaling, given the smallness of the a-value. Thus, when hypothesised relationships were not significant as power law relationships, we tested linear regressions, and report these when significant; this was the case for the scaling of the parenchymatous bundle sheath and the lower epidermis, and, for C_3 species only, the scaling of the mestome sheath and the upper epidermis (Figure 3).

We utilised a trimmed phylogeny to test relationships with the parenchymatous bundle sheath, which was possessed by only 21 of the grass species (Supporting Information: Figure S1; that is, all C_3 and C_4 species with three longitudinal vein orders). Finally, analyses including second order vein or sheath traits excluded the species *L. sorghoidea*, and trimmed phylogenies excluding this species were also implemented.

3 | RESULTS

3.1 | Diversity in grass leaf cell and tissue anatomy

Grass species varied strongly in the mean cell cross-sectional areas of all tissues, from fourfold for type II xylem conduits to 17-fold for parenchymatous bundle sheath cells, and in leaf dimensions, from threefold for thickness to 24-fold for leaf width (Supporting Information: Table S1). On average, 76% of trait variation was explained by differences among species rather than among individuals in each species (ANOVA; Supporting Information: Table S2, Supporting Information: Figures S2 and S3). C_4 species had larger cell areas on average than C_3 for the upper epidermis, mestome sheath, and 3° vein xylem (phylogenetic ANOVAs; Supporting Information: Table S2).

3.2 | Anatomical allometries of cell sizes across tissues

We found allometries among cell sizes across tissues for 15 of the 21 pairwise combinations of tissues, that is, the lower and upper

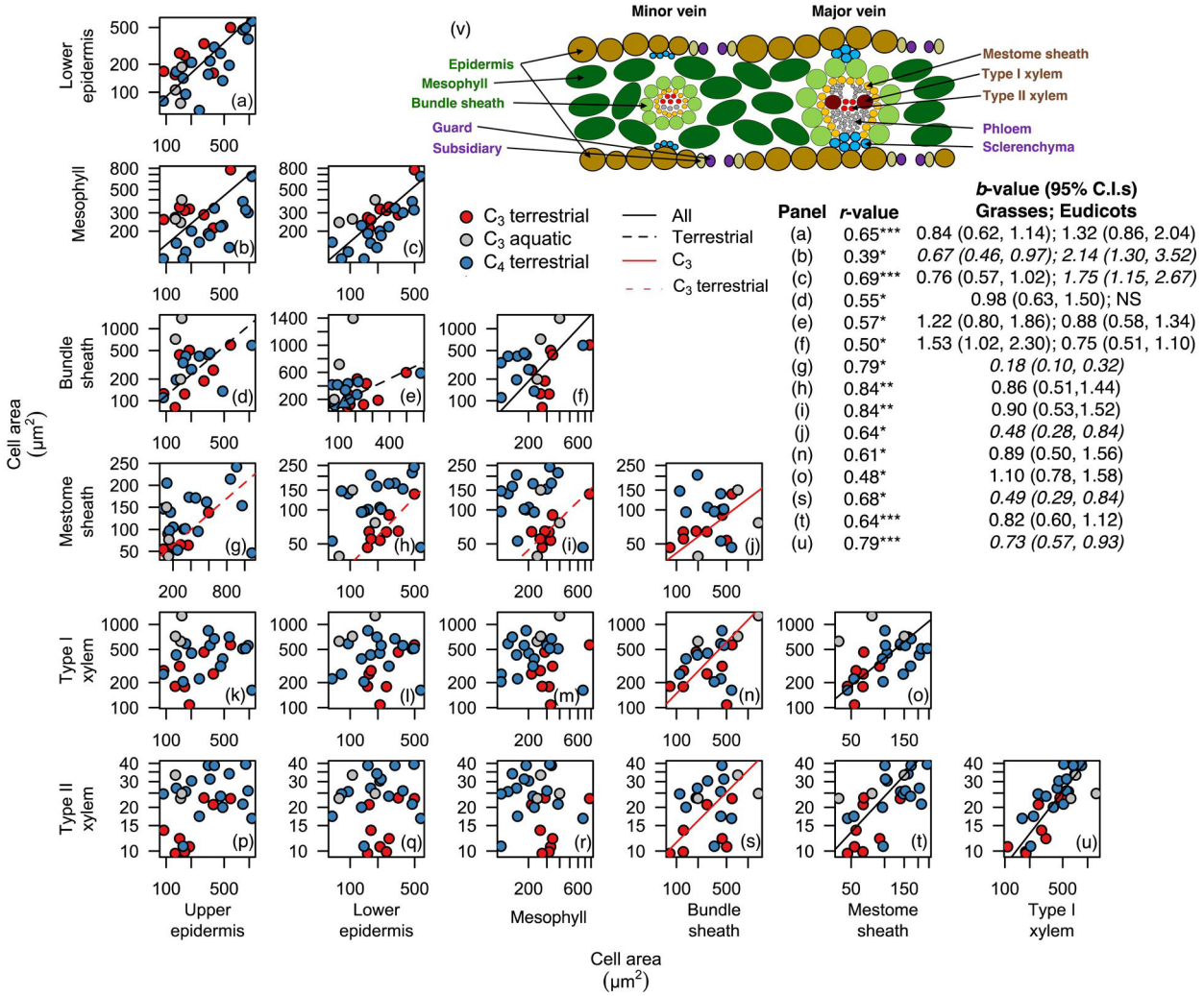

FIGURE 3 Grass cell size allometries and anatomy. (a–u) Allometries across tissues of grass leaves. (v) Schematic of C_3 grass cross-sectional anatomy. Green and brown labels in (v) represent cells derived from non-procambium and procambium precursor cells, respectively (unmeasured cells in purple). Each point is one species, $n = 11$ C_3 (eight terrestrial in red, three aquatic in grey) and $n = 16$ C_4 species in blue. Fitted lines are phylogenetic reduced major axis (PRMA) regressions with statistics on the right and in Supporting Information: Table S3. Line colours indicate that the relationship was significant across a specific set of grasses, with black lines across all species, red lines across C_3 species, and segmented lines across the terrestrial species either across all grasses or only C_3 grasses. *b*-values are presented for grasses and eudicots; italics indicate departure from geometric scaling. See Table 1 for cell type definitions. $^*p < 0.05$, $^{**}p < 0.01$, $^{***}p < 0.001$. [Color figure can be viewed at wileyonlinelibrary.com]

epidermis, mesophyll, parenchymatous bundle and mestome sheaths, and type I and type II xylem (phylogenetic reduced major axis; Figure 3). The allometries between epidermises, for epidermises versus mesophyll, for parenchymatous bundle sheath versus mesophyll, between xylem types, and for xylem versus mestome sheath were significant across all species. However, several relationships involving xylem, epidermises and vein sheaths, were significant only for the terrestrial grasses or the terrestrial C_3 grasses (Figure 3; Supporting Information: Figure S5, Supporting Information: Tables S3 and S4). Xylem cell sizes were statistically independent of those in mesophyll and epidermises. Within vein orders, significant relationships arose for 14 of the 16 allometries, that is, among parenchymatous bundle and mestome sheaths and type I and II xylem (Figure 4 and Supporting Information: Figures S4 and S5; Supporting Information: Table S4).

Cell size allometries were geometric for 10 of the 15 significant across-tissue relationships and for 8 of the 14 significant within-vein relationships ($b = 1$). Nongeometric allometries across-tissues were those of mesophyll versus upper epidermis, mesophyll versus parenchymatous bundle sheath, type I versus type II xylem, parenchymatous bundle sheath versus mestome sheath and parenchymatous bundle sheath versus type II xylem. Non-geometric relationships within-veins were those of type I versus type II xylem, mestome sheath versus type I xylem, and parenchymatous bundle sheath versus type II xylem (all within the 1° vein), and mestome sheath versus parenchymatous bundle sheath (within the 1°, 2°, and 3° veins; Supporting Information: Tables S3 and S4).

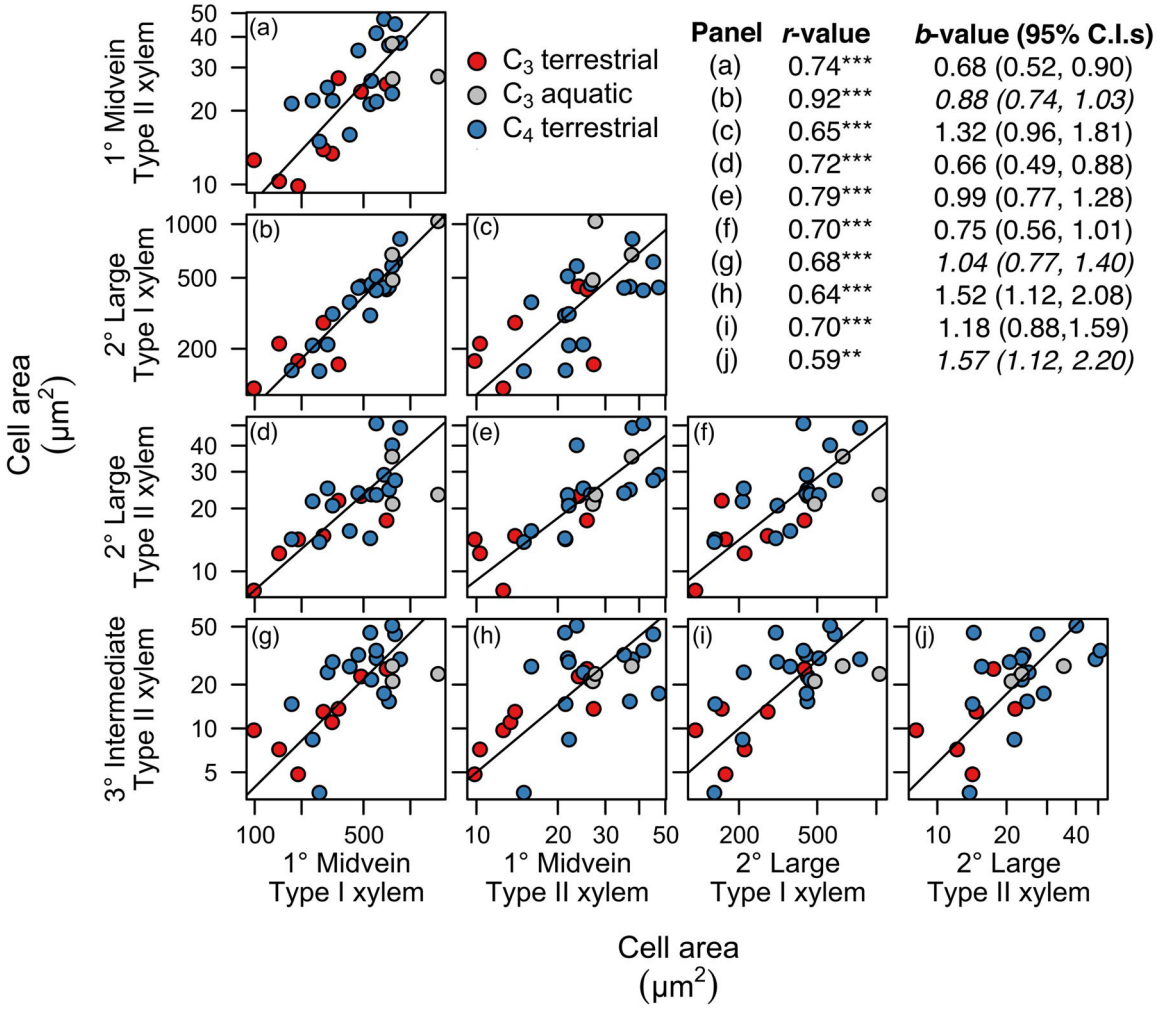

FIGURE 4 Allometries of xylem cells within and across vein orders. Each point is one species, $n = 11$ C_3 (eight terrestrial in red, three aquatic in grey) and $n = 16$ C_4 species in blue. Allometries for 4° xylem with cell types of other vein orders were not significant and are omitted (see Supporting Information: Table S4). Lines were fitted with phylogenetic reduced major axis regressions (PRMA) and statistics and parameters are found in Supporting Information: Table S4. Italics indicate departure from geometric scaling. See Table 1 for cell type definitions. $^{*}p < 0.05$, $^{**}p < 0.01$, $^{***}p < 0.001$. [Color figure can be viewed at wileyonlinelibrary.com]

3.3 | Allometries among cell, leaf and plant dimensions

Across species, leaf dimensions and plant height were positively related to leaf cell sizes in all tissues (Figures 5–6; Supporting Information: Table S5; Supporting Information: Figure S6). Thus, leaf thickness was allometrically linked with cell areas in the mesophyll and epidermises; leaf width was allometrically linked with cell areas in the mesophyll, parenchymatous bundle sheath and type I xylem (Figure 5); and leaf area was allometrically linked with cell area in the lower epidermis. Further, leaf length, leaf area and plant size (culm height) were allometrically linked with cell areas in the type I and II xylem; leaf length and leaf area with cell areas in the mestome sheath; and culm height with cell areas of the parenchymatous bundle sheath (Figure 6). The majority of allometries held across all species, but several relationships involving the epidermises and vein tissues were significant only for the terrestrial grasses or the terrestrial C_3 grasses (Figures 5 and 6). The allometries of leaf thickness versus cell areas were geometric, whereas the majority of the relationships of leaf width, leaf length, leaf area and culm height versus cell areas were greater than geometric (Figures 5 and 6; Supporting Information: Table S5).

3.4 | Contrasting anatomical allometries of grasses and eudicots

Grasses showed similar allometries between cell sizes for lower epidermis versus upper epidermis and the parenchymatous bundle sheath as previously found for diverse eudicots (Figure 2; John et al., 2013) However, grasses differed from eudicots for allometries between cell sizes for the mesophyll versus the parenchymatous bundle sheath ($b < 1$ for grasses; $b = 1$ for eudicots), and for mesophyll versus epidermises ($b < 1$ and $b = 1$ with the lower and upper

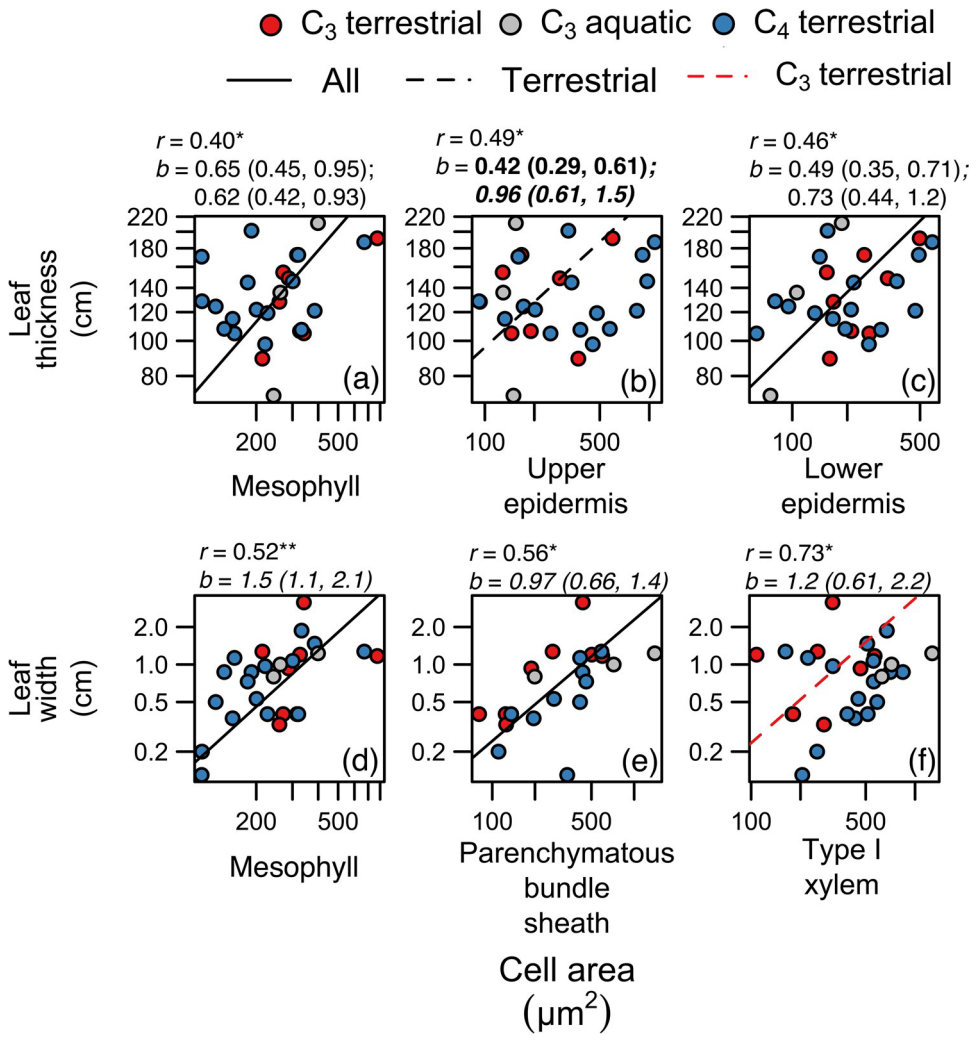

FIGURE 5 Allometries of leaf morphological dimensions with leaf cell size as building blocks. (a–f) Allometries of leaf with leaf cell areas within tissues of grass leaves. Each point is one species, $n = 11$ C_3 (eight terrestrial in red, three aquatic in grey) and $n = 16$ C_4 species in blue. Fitted lines are phylogenetic reduced major axis (PRMA) regressions with statistics above each panel and in Supporting Information: Table S5. Line colours indicate that the relationship was significant across a specific set of grasses, with black lines across all species, red lines across C_3 species, and segmented lines across the terrestrial species either across all grasses or only C_3 grasses. *b*-values are presented for grasses and eudicots for comparisons with leaf thickness and bolded when significantly different; italics indicate departure from geometric scaling. See Figure 3 and Table 1 for cell type definitions. $^*p < 0.05$, $^{**}p < 0.01$. [Color figure can be viewed at wileyonlinelibrary.com]

epidermis respectively in grasses; $b > 1$ for both in eudicots; Figure 3), and for leaf thickness versus cell areas of the upper epidermis ($b = 0.5$ for grasses; $b > 0.5$ for eudicots; Figure 5b).

3.5 | Allometric coordination of cell sizes with light-saturated photosynthetic rates and other functional traits

Across species, cell sizes were associated positively with mass-based light-saturated photosynthetic rates (A_{mass}) and its determinants, the area-based light-saturated photosynthetic rate (A_{area}) and negatively associated with *LMA*. Cell sizes were also associated negatively with the major vein length per area (VLA_{major}) (Figure 7; Supporting Information: Figure S7; Supporting Information: Table S6). A_{mass} was generally positively coordinated with the mean cross-sectional areas of cells in all tissues; however, the association with mesophyll cell size was significant only for C_4 species, and marginally nonsignificant for C_3 species alone or for all species pooled (Supporting Information: Table S6). Compared with the majority of C_3 grasses included in this study C_4 grasses achieved higher A_{mass} for a given mesophyll cell size (Figure 7). C_4 species had significantly higher A_{area}, and the similar investment in *LMA* between C_3 and C_4 species resulted in C_4 species also having higher A_{mass} (Supporting Information: Table S2). A_{area} was correlated with fewer cell cross-sectional areas than A_{mass}, showing significant associations with those of the upper epidermis (terrestrial species only), mestome sheath, and type I and II xylem

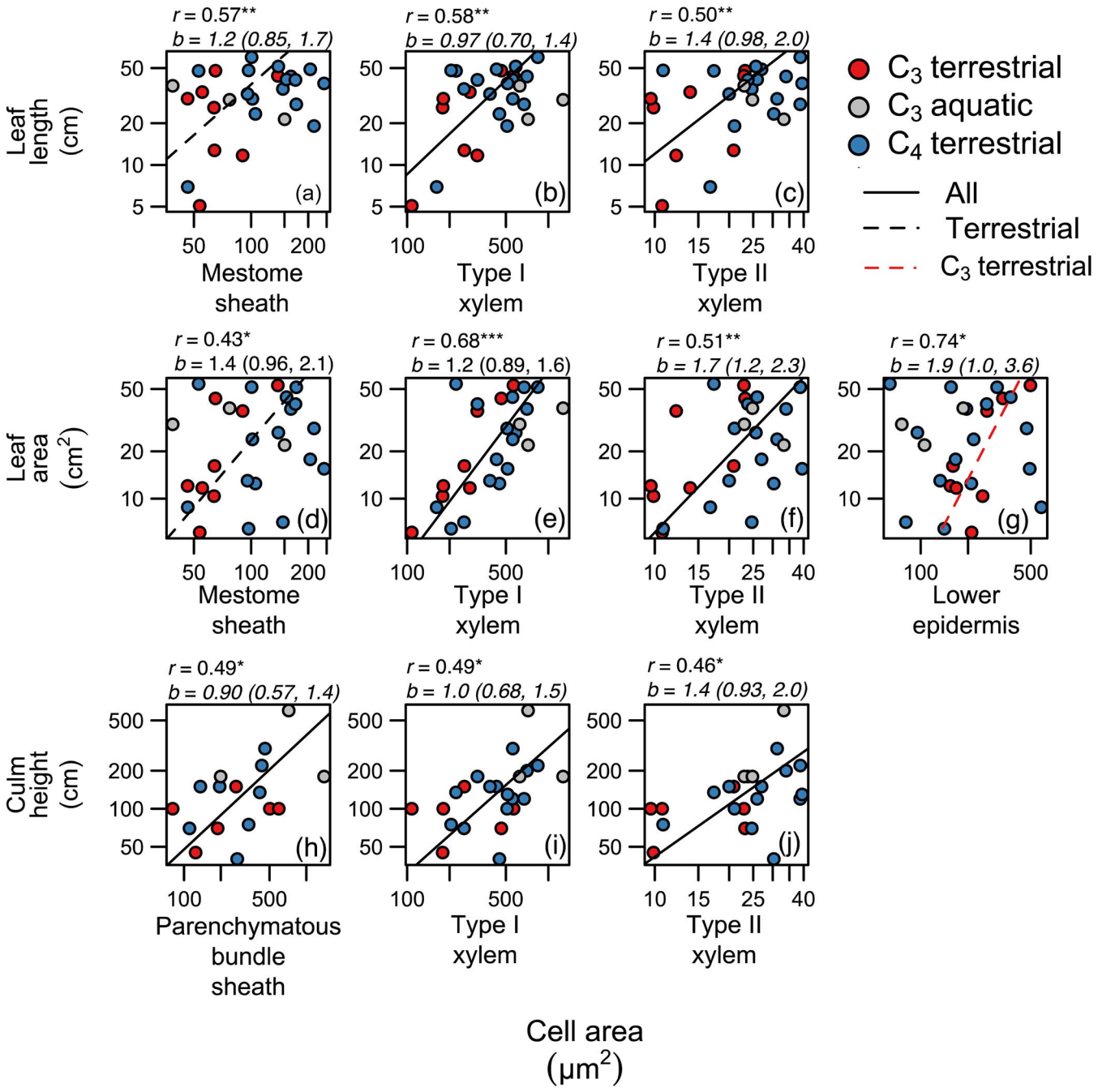

FIGURE 6 Allometries of leaf morphological and plant dimensions with leaf cell size for hydraulic design. (a–j) Allometries of leaf and plant dimensions with leaf cell areas within tissues of grass leaves. Each point is one species, $n = 11$ C_3 (eight terrestrial in red, three aquatic in grey) and $n = 16$ C_4 species in blue. Fitted lines are phylogenetic reduced major axis (PRMA) regressions with statistics above each panel and in Supporting Information: Table S5. Line colours indicate that the relationship was significant across a specific set of grasses, with black lines across all species, red lines across C_3 species, and segmented lines across the terrestrial species either across all grasses or only C_3 grasses. *b*-values are presented for grasses and eudicots for comparisons with leaf thickness and bolded when significantly different; italics indicate departure from geometric scaling. See Figure 3 and Table 1 for cell type definitions. $^*p < 0.05$, $^{**}p < 0.01$, $^{***}p < 0.001$. [Color figure can be viewed at wileyonlinelibrary.com]

(Supporting Information: Figure S7b,e–g). *LMA* was negatively related to the cross-sectional areas of the mesophyll, bundle sheath, and lower epidermis across all species, and additionally to cell areas in the upper epidermis when considering only C_4 species, but was not linked with cell areas in the mestome sheath and xylem. Finally, VLA_{major} was negatively related to the cross-sectional areas of just the mesophyll and bundle sheath (Supporting Information: Figure S7h–k,o,r).

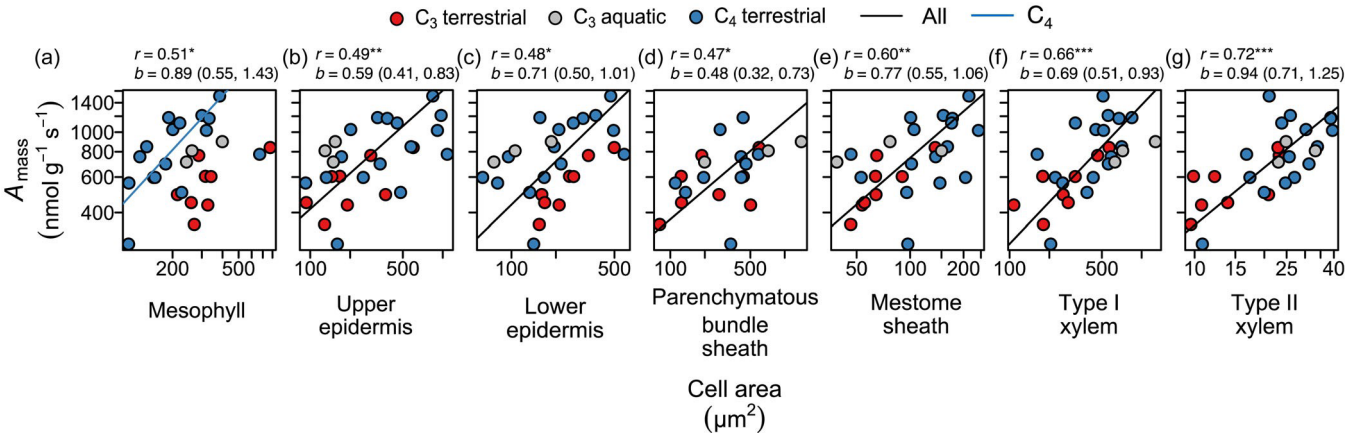

FIGURE 7 Allometries of mass-based photosynthetic rate with leaf cell size. (a–g) Allometries of light-saturated mass-based leaf photosynthetic rate with leaf cell areas within tissues of grass leaves. Each point is one species, $n = 11$ C_3 (eight terrestrial in red, three aquatic in grey) and $n = 16$ C_4 species in blue. Fitted lines are phylogenetic reduced major axis (PRMA) regressions with statistics above each panel and in Supporting Information: Table S6. Line colours indicate that the relationship was significant across a specific set of grasses, with black lines across all species and the blue line in (a) across only C_4 species. See Figure 3 and Table 1 for cell type definitions. $^*p < 0.05$, $^{**}p < 0.01$, $^{***}p < 0.001$. [Color figure can be viewed at wileyonlinelibrary.com]

4 | DISCUSSION

Allometries across the morphological and anatomical diversity of C_3 and C_4 grass leaves suggest conserved developmental processes and functional coordination of cell sizes and organ and plant dimensions, with implications for leaf and plant design and function (Figures 3–7).

4.1 | Allometries of cell sizes: Patterns across tissues, and contrasts between C_3 and C_4 grasses

While Kranz anatomy of C_4 species meant that C_3 and C_4 species differed strongly in their anatomy, many allometries were conserved across the two photosynthetic types (Figures 3–7; Table 2). Across-species allometries between cell areas within and among tissues would emerge from conserved coordinated cell expansion within organs (Granier & Tardieu, 1998; Volkenburgh, 1999), reinforced by selection for proportional cell sizes (and possibly cell numbers) that would facilitate coordination of metabolic and transport functions within and across tissues (Brodribb et al., 2013; Cadart & Heald, 2022; John et al., 2013). Generally, cell area allometries occurred among cells derived from the same developmental precursors (Table 1). Thus, we found cell size allometries for cells arising from lamina precursor cells, including epidermises, mesophyll and the parenchymatous bundle sheath (Figure 3a–f). Separately, we found independent cell size allometries for cells arising from the procambium, including xylem and mestome sheath (Figure 3o,t–u).

We note that our study did not include a focus on phloem cells, which also arise from procambium precursors. Elucidating potential allometries of phloem with other cell types and whole plant design remains an urgent avenue for future research linking sugar transport with leaf and whole plant function (Hölttä et al., 2013; Ronellenfitsch et al., 2015).

Beyond the allometries that could be explained by shared developmental precursor cells, we found that C_3 species showed more generalised scaling of cell areas across tissues than C_4 species (Figure 3 and Supporting Information: Figures S4 and S5; Supporting Information: Table 2). For C_3 species, we found allometries between cells that arose from different precursors, that is, cells of mestome sheath versus mesophyll, epidermis and parenchymatous bundle sheath, and xylem versus parenchymatous bundle sheath cells (Figure 3g–j,n,s). Allometries among cells arising from different developmental precursors in C_3 species suggest selection for coordination of metabolism and transport (Brodribb et al., 2013). In the C_4 species, the independence of cell sizes of the parenchymatous bundle sheath from xylem, and mestome sheath from mesophyll, is consistent with the additional constraints imposed by their Kranz anatomy, including the necessity for large sheath cells, irrespective of mesophyll cell sizes (Christin et al., 2013). The large C_4 sheath cells, with specialised metabolism and transport, have much more extensive plasmodesmatal connections with the mesophyll than sheath cells of C_3 species, which presumably act as an alternative to coordination of cell size and interfacing cell surface areas for transport function (Cadart & Heald, 2022; Christin et al., 2013; Danila et al., 2016).

We found several allometries that occurred only among terrestrial grasses, including the relationships of cell sizes in the parenchymatous bundle sheath versus upper and lower epidermises. Overall, the aquatic species had consistently smaller epidermal cells than terrestrial grasses, potentially reflecting their generally less pronounced water storage and potentially a lower requirement for large bulliform cells that enables leaves to roll and thereby better

avoid overheating and dehydrating under dry conditions (Ellis, 1976; Evert, 2006).

4.2 | Allometries among cell, leaf and plant dimensions: Cells as building blocks and hydraulic design

We found strong allometries between leaf dimensions and the sizes of their constituent cells (Figure 5; Table 2). Cell sizes (in addition to cell numbers) may make especially important contributions to leaf dimensions especially given the low airspace porosity of grass leaves (Supporting Information: Figures S2 and S3; Gázquez and Beemster, 2017). Thus, thicker grass leaves are associated with larger cells in the mesophyll and epidermises, and wider leaves with larger mesophyll and parenchymatous bundle sheath cells (Figure 5 and Supporting Information: Figure S6). Notably, the scaling of leaf width with the cell sizes in the mesophyll and the parenchymatous bundle sheath provides an anatomical mechanism for the global relationship of lower VLA_{major} in wider grass leaves (Baird et al., 2021). The major veins are patterned early by the procambium and thus greater mesophyll and parenchymatous bundle sheath cell expansion would space major veins further apart in wider leaves (Baird et al., 2021), a pattern supported by the negative relationship of VLA_{major} with cell sizes in those tissues (Supporting Information: Figure S7). Thus, the allometric linkages of cell size and leaf dimensions enables stress tolerance traits to be selected across levels of organisation as smaller cells and narrower leaves, both linked with higher vein densities, would contribute to tolerance of drought (Baird et al., 2021; Cutler et al., 1977).

We found strong allometries of xylem cell sizes with leaf length, leaf area and plant height (Figure 6; Table 2). These relationships are consistent with selection of larger xylem cells for greater biomechanical support, and hydraulic capacity to mitigate both the greater pathlength in longer leaves and the potentially higher evaporative loads in larger plants. Indeed, these trends are consistent with global trends for the scaling of plant height with xylem conduit sizes in the stems of taller plants, including trees (Figure 5h,i,k-l,o,p; Baird et al., 2021; Olson et al., 2018; Sack et al., 2013). Likewise, the larger parenchymatous bundle sheath cells in leaves of taller grasses may provide greater storage and outside-xylem hydraulic conductance that would contribute to mitigating the hydraulic stresses associated with both larger plant size and greater exposure and thus, higher evaporative demand (Figure 5n; Buckley et al., 2015).

Geometric scaling was typical for the allometric relationships of cell sizes across grass species. Geometric scaling is consistent with both proportional cell expansion, and coordination of cell sizes for matched flows of water, nutrients and sugars (Brodribb et al., 2013; Cadart & Heald, 2022; Granier & Tardieu, 1998; John et al., 2013; Volkenburgh, 1999). The cases in which specific allometries departed from geometric scaling could be explained based on specific developmental causes and functional benefits for the disproportionate size of one cell type over another (Table 3). For example, the greater increase in cell sizes in the parenchymatous bundle sheath and upper epidermis relative to the mesophyll ($b > 1$) is consistent with a disproportionate investment in support functions including water storage in epidermises, and bundle sheath (Griffiths et al., 2013) and for epidermal bulliform cells influencing mechanical protection and leaf rolling during dehydration (Ellis, 1976; Evert, 2006), which would protect leaves with larger mesophyll cells (Figure 3b,f). Further, the less-than-geometric scaling in the cell size of type II relative to type I xylem ($b < 1$) is consistent with the optimisation of vascular system design, as type I xylem are present only in major vein orders, which decline in vein length per area in wider leaves (Figure 3u; Table 3; Baird et al., 2021). Thus, a disproportionate increase in type I relative to type II xylem cell size would compensate at least in part for the effect of declining vein length per area of major veins on vein transport efficiency and also provide greater mechanical rigidity (Table 3). Several of the allometries of leaf and plant dimensions with cell areas exhibited greater-than-geometric scaling, which would arise for several reasons. First, the greater than geometric scaling of leaf width with the cell areas of mesophyll and the parenchymatous bundle sheath ($b > 0.5$) is consistent with wider leaves being determined by greater cell numbers even more than by larger cells, with a particular role of the larger diameter veins in wider leaves (Figure 5; Table 3; Gázquez & Beemster, 2017; John et al., 2017; Pantin et al., 2012). This contrasts with the geometric scaling of leaf thickness with the cell areas of mesophyll and the epidermises, which indicates a greater role for cell size than cell number in driving thickness differences. Further, the greater-than-geometric scaling of leaf length, leaf area and culm height with xylem cell areas ($b > 0.5$ for leaf length and culm height, $b > 1$ for leaf area) is consistent with optimisation of the vascular system design, as hydraulic conductance through xylem conduits increases as a function of the radius to the fourth power, so xylem would not need to increase proportionally in size to counteract the impact of increasing path length in longer leaves and taller grass shoots (Nobel, 2020).

4.3 | Contrasting leaf allometries align with key morphological divergences between grasses and eudicots

Grasses and eudicots were similar in several anatomical allometries, including geometric scaling of cell areas of the epidermises, and of the lower epidermis versus the parenchymatous bundle sheath, consistent with coordinated development and function (Figures 3, 5, and 6; Table 2). However, several trends differed for grasses. The scaling of xylem cell sizes with leaf dimensions in grasses, not observed for eudicots, is consistent with the specific importance of cell sizes for biomechanical support and axial hydraulic transport in longer grass leaves (Figure 6). The less than geometric scaling of cell areas of mesophyll versus upper epidermis in grasses, but geometric scaling in eudicots, is consistent with many grass leaves investing in large bulliform cells for storage and leaf rolling movements, a

specialisation typically not observed in eudicots (Figure 1b; Table 3). The geometric scaling of leaf thickness versus cell area of the upper epidermis in grasses, but greater than geometric scaling in eudicots, indicates coordinated contribution of cell size to leaf thickness in grasses and a greater contribution of cell layers to thickness in eudicots. This is consistent with eudicot leaves having many palisade layers and the lower proportion of airspace in grass leaves relative to eudicots (Figure 5, Supporting Information: Figures S2 and S3). While these differences between grasses and eudicots are consistent with their contrasting structure, sampling additional diversity will improve our ability to generalise; for example, we do not know whether the trends we report here for grasses are generalisable more broadly to monocots. Further, it may be possible to resolve similar allometries in some eudicot lineages, depending on taxonomic scale.

4.4 | Allometric scaling of photosynthetic rate with cell size in grasses

Across grass species, light-saturated photosynthetic rate was strongly related to cell sizes. Our data provide a novel resolution of the relationship across grass species of A_{mass} with coordinated changes in cell cross-sectional size across the mesophyll, epidermises, parenchymatous bundle sheath, mestome sheath, and type I and II xylem (Figure 7; Table 2). That photosynthetic rate coordinates with cell size across cell types indicates that the separate allometries between procambium and nonprocambium derived cell types converge to maximise photosynthetic function (Figure 7; Supporting Information: Figure S7).

Notably, light-saturated photosynthetic rate can be limited by many factors (Niinemets et al., 2009; Salvi et al., 2021), and A_{mass} in particular is influenced by structural relative to photosynthetic allocation. Leaves with high A_{mass} allocate more mass to photosynthetic structure relative to structural components that increase leaf longevity (Wright et al., 2004); thus, a higher A_{mass} can arise from a higher A_{area} and/or lower *LMA* (Sack et al., 2013). We expected that larger-celled leaves would have higher A_{mass}, not due to direct causality but from several structural effects. First, larger cells, and particularly larger cells in the mesophyll (Figure 5a), were associated with thicker leaves, as found for eudicots (John et al., 2017) and would correspond to a higher number of chloroplasts (Ellis & Leech, 1985) and a higher concentration of photosynthetic machinery per leaf area (Garnier et al., 1999; Koike, 1988) and thus, a higher A_{area} (Niinemets, 1999). Second, we expected that small cells would be related to higher *LMA* through a higher concentration of cell wall material per leaf area (John et al., 2017), and, as $A_{mass} = A_{area}/LMA$, this higher *LMA* would correspond to a lower A_{mass} for small-celled species. Indeed, we found that higher *LMA* was related to smaller cell size in several tissues, including the mesophyll, epidermises and parenchymatous bundle sheath (Supporting Information: Figure S7). Third, VLA_{major} may also contribute substantially to higher *LMA* (John et al., 2017; Sack et al., 2013), and small mesophyll and bundle sheath cells were associated with more closely-spaced veins and thus higher VLA_{major}. While a higher VLA_{major} is implicated in hydraulic function and contributes to higher A_{area} in grasses (Baird et al., 2021), across species, the contribution of high VLA_{major} to a higher *LMA* in small-celled species would contribute to a low A_{mass} in small-celled species, and higher A_{mass} in large-celled species. Finally, the association of higher A_{area} with larger type I and type II xylem conduits (Supporting Information: Figure S7) is consistent with these larger conduits providing greater hydraulic supply that enables greater stomatal opening and higher photosynthetic gas exchange (Sack & Scoffoni, 2013). Thus, the association between A_{mass} and cell sizes in all tissues are consistent with multiple expected impacts of cell size on A_{area} and/or *LMA* (Supporting Information: Figure S7). The possibility that cell size is a relatively simple predictor of mass normalised photosynthetic productivity in grasses is a finding with potential applications both in understanding the ecology of diverse grass species and for improving crop productivity.

5 | CONCLUSION

Anatomical allometries across grass leaves shown theoretically and empirically in this study highlight the critical role of developmental processes in driving allometries across species, but should be explored in future studies focused at the level of cell development within and across species, for example, identifying the genetic regulators of differences in cell size within the model grass *Brachypodium*. The strong patterns demonstrated show how leaf construction emerges from differences at the level of cells that cascade upwards to tissues, organs, and through linkages with photosynthetic efficiency, potentially to whole plant form and function. Future studies should resolve whether allometric scaling patterns determined here are generalisable across further diversity in the grass family by sampling additional C_3 and C_4 lineages across the grass phylogeny (e.g., C_3 Pooid, PCK C_4, bamboos), and other monocots.

ACKNOWLEDGEMENTS

We thank T. Cheng, W. Deng, A. C. Diener, A. Kooner, M. McMaster, C. D. Medeiros, S. Moshrefi, L. A. Nikolov, A. J. Patel, V. M. Savage, A. Sayari, E. Scarpella, and F. Zapata for logistical assistance. Funding was provided by the US National Science Foundation (grants 1457279, 1951244, 2017949 and 1943583) and the Natural Environment Research Council (grants NE/DO13062/1 and NE/T000759/1).

CONFLICT OF INTEREST STATEMENT

The authors declare no conflict of interest.

DATA AVAILABILITY STATEMENT

The data that supports the findings of this study are available in the supplementary material of this article. Data are available in the electronic supplementary material. Code used for analyses was previously published and available on GitHub (Baird et al., 2021).

ORCID

Alec S. Baird http://orcid.org/0000-0002-9859-5633
Samuel H. Taylor http://orcid.org/0000-0001-9714-0656
Teera Watcharamongkol http://orcid.org/0000-0002-3065-8597
Grace P. John http://orcid.org/0000-0002-8045-5982
Christine Scoffoni http://orcid.org/0000-0002-2680-3608
Colin P. Osborne http://orcid.org/0000-0002-7423-3718
Lawren Sack http://orcid.org/0000-0002-7009-7202

REFERENCES

Baird, A.S., Taylor, S.H., Pasquet-Kok, J., Vuong, C., Zhang, Y., Watcharamongkol, T. et al. (2021) Developmental and biophysical determinants of grass leaf size worldwide. *Nature*, 592, 242–247.

Beer, C., Reichstein, M., Tomelleri, E., Ciais, P., Jung, M., Carvalhais, N. et al. (2010) Terrestrial gross carbon dioxide uptake: global distribution and covariation with climate. *Science*, 329, 834–838.

Brodribb, T.J., Jordan, G.J. & Carpenter, R.J. (2013) Unified changes in cell size permit coordinated leaf evolution. *New Phytologist*, 199, 559–570.

Buckley, T.N., John, G.P., Scoffoni, C. & Sack, L. (2015) How does leaf anatomy influence water transport outside the xylem? *Plant Physiology*, 168, 1616–1635.

Cadart, C. & Heald, R. (2022) Scaling of biosynthesis and metabolism with cell size. *Molecular Biology of the Cell*, 33, pe5.

Charles-Edwards, D.A., Charles-Edwards, J. & Sant, F.I. (1974) Leaf photosynthetic activity in six temperate grass varieties grown in contrasting light and temperature environments. *Journal of Experimental Botany*, 25, 715–724.

Christin, P.-A., Osborne, C.P., Chatelet, D.S., Columbus, J.T., Besnard, G., Hodkinson, T.R. et al. (2013) Anatomical enablers and the evolution of C_4 photosynthesis in grasses. *Proceedings of the National Academy of Sciences United States of America*, 110, 1381–1386.

Clayton, W., Vorontsova, M., Harman, K. & Williamson, H. (2006) *RBG Kew: GrassBase—The online world grass flora*. https://www.kew.org/data/grasses-db.html?

Clevering, O.A. (1999) Between- and within-population differences in *Phragmites australis*. *Oecologia*, 121, 447–457.

Cutler, J.M., Rains, D.W. & Loomis, R.S. (1977) The importance of cell size in the water relations of plants. *Physiologia Plantarum*, 40, 255–260.

Danila, F.R., Quick, W.P., White, R.G., Furbank, R.T. & von Caemmerer, S. (2016) The metabolite pathway between bundle sheath and mesophyll: quantification of plasmodesmata in leaves of C_3 and C_4 monocots. *The Plant Cell*, 28, 1461–1471.

Dannenhoffer, J.M., Ebert, Jr. W. & Evert, R.F. (1990) Leaf vasculature in barley, *Hordeum Vulgare* (poaceae). *American Journal of Botany*, 77, 636–652.

Dengler, N.G., Dengler, R.E. & Hattersley, P.W. (1985) Differing ontogenetic origins of PCR ("Kranz") sheaths in leaf blades of C_4 grasses (Poaceae). *American Journal of Botany*, 72, 284–302.

Eckardt, N.A., Ainsworth, E.A., Bahuguna, R.N., Broadley, M.R., Busch, W., Carpita, N.C. et al. (2023) Climate change challenges, plant science solutions. *The Plant Cell*, 35, 24–66.

Ellis, J.R. & Leech, R.M. (1985) Cell size and chloroplast size in relation to chloroplast replication in light-grown wheat leaves. *Planta*, 165, 120–125.

Ellis, R.P. (1976) A procedure for standardizing comparative leaf anatomy in the Poaceae. I. the leaf-blade as viewed in transverse section. *Bothalia*, 12, 65–109.

Ermakova, M., Danila, F.R., Furbank, R.T. & von Caemmerer, S. (2020) On the road to C_4 rice: advances and perspectives. *The Plant Journal*, 101, 940–950.

Evert, R.F. (2006) *Esau's plant anatomy: meristems, cells, and tissues of the plant body: their structure, function, and development*. Hoboken, New Jersey: John Wiley & Sons.

Fletcher, L.R., Cui, H., Callahan, H., Scoffoni, C., John, G.P., Bartlett, M.K. et al. (2018) Evolution of leaf structure and drought tolerance in species of Californian Ceanothus. *American Journal of Botany*, 105, 1672–1687.

Fournier, C., Durand, J.L., Ljutovac, S., Schäufele, R., Gastal, F. & Andrieu, B. (2005) A functional-structural model of elongation of the grass leaf and its relationships with the phyllochron. *New Phytologist*, 166, 881–894.

Garland, Jr. T., Dickerman, A.W., Janis, C.M. & Jones, J.A. (1993) Phylogenetic analysis of covariance by computer simulation. *Systematic Biology*, 42, 265–292.

Garnier, E., Salager, J.-L., Laurent, G. & Sonie, L. (1999) Relationships between photosynthesis, nitrogen and leaf structure in 14 grass species and their dependence on the basis of expression. *New Phytologist*, 143, 119–129.

Gázquez, A. & Beemster, G.T.S. (2017) What determines organ size differences between species? A meta-analysis of the cellular basis. *New Phytologist*, 215, 299–308.

Granier, C. & Tardieu, F. (1998) Spatial and temporal analyses of expansion and cell cycle in sunflower leaves[1]. *Plant Physiology*, 116, 991–1001.

Granier, C. & Tardieu, F. (2009) Multi-scale phenotyping of leaf expansion in response to environmental changes: the whole is more than the sum of parts. *Plant, Cell & Environment*, 32, 1175–1184.

Griffiths, H., Weller, G., Toy, L.F. & Dennis, R.J. (2013) You're so vein: bundle sheath physiology, phylogeny and evolution in C_3 and C_4 plants. *Plant, Cell & Environment*, 36, 249–261.

Hölttä, T., Kurppa, M. & Nikinmaa, E. (2013) Scaling of xylem and phloem transport capacity and resource usage with tree size. *Frontiers in Plant Science*, 4, 1–19.

Huxley, J.S. (1932) *Problems of relative growth*. Baltimore, MD: John Hopkins University Press.

John, G.P., Scoffoni, C., Buckley, T.N., Villar, R., Poorter, H. & Sack, L. (2017) The anatomical and compositional basis of leaf mass per area. *Ecology Letters*, 20, 412–425.

John, G.P., Scoffoni, C. & Sack, L. (2013) Allometry of cells and tissues within leaves. *American Journal of Botany*, 100, 1936–1948.

Kato, Y. & Okami, M. (2010) Root growth dynamics and stomatal behaviour of rice (*Oryza sativa* L.) grown under aerobic and flooded conditions. *Field Crops Research*, 117, 9–17.

Kemp, C.D. (1960) Methods of estimating the leaf area of grasses from linear measurements. *Annals of Botany*, 24, 491–499.

Koike, T. (1988) Leaf structure and photosynthetic performance as related to the forest succession of deciduous broad-leaved trees1. *Plant Species Biology*, 3, 77–87.

Lowry, D.B., Lovell, J.T., Zhang, L., Bonnette, J., Fay, P.A., Mitchell, R.B. et al. (2019) QTL × environment interactions underlie adaptive divergence in switchgrass across a large latitudinal gradient. *Proceedings of the National Academy of Sciences United States of America*, 116, 12933–12941.

McSteen, P. & Kellogg, E.A. (2022) Molecular, cellular, and developmental foundations of grass diversity. *Science*, 377, 599–602.

Meinzer, F.C., James, S.A., Goldstein, G. & Woodruff, D. (2003) Whole-tree water transport scales with sapwood capacitance in tropical forest canopy trees. *Plant, Cell & Environment*, 26, 1147–1155.

Nelson, T. & Dengler, N. (1997) Leaf vascular pattern formation. *The Plant Cell*, 9, 1121–1135.

Niinemets, Ü. (1999) Research review: components of leaf dry mass per area-thickness and density-alter leaf photosynthetic capacity in reverse directions in woody plants. *New Phytologist*, 144, 35–47.

Niinemets, Ü., Díaz-Espejo, A., Flexas, J., Galmés, J. & Warren, C.R. (2009) Role of mesophyll diffusion conductance in constraining potential photosynthetic productivity in the field. *Journal of Experimental Botany*, 60, 2249–2270.

Niklas, K.J. (1994) *Plant Allometry*. Chicago, IL: University of Chicago Press.

Nobel, P.S. (1976) Photosynthetic rates of sun versus shade leaves of *Hyptis emoryi* Torr. *Plant Physiology*, 58, 218–223.

Nobel, P.S. (2020) *Physicochemical and environmental plant physiology*, 5th ed. San Diego, CA: Academic Press.

Nobel, P.S., Zaragoza, L.J. & Smith, W.K. (1975) Relation between mesophyll surface area, photosynthetic rate, and illumination level during development for leaves of *Plectranthus parviflorus* Henckel. *Plant Physiology*, 55, 1067–1070.

Olson, M.E., Soriano, D., Rosell, J.A., Anfodillo, T., Donoghue, M.J., Edwards, E.J. et al. (2018) Plant height and hydraulic vulnerability to drought and cold. *Proceedings of the National Academy of Sciences United States of America*, 115, 7551–7556.

Pantin, F., Simonneau, T. & Muller, B. (2012) Coming of leaf age: control of growth by hydraulics and metabolics during leaf ontogeny. *New Phytologist*, 196, 349–366.

Poorter, H. & Sack, L. (2012) Pitfalls and possibilities in the analysis of biomass allocation patterns in plants. *Frontiers in Plant Science*, 3, 1–10.

Revell, L.J. (2012) phytools: an R package for phylogenetic comparative biology (and other things): phytools: R package. *Methods in Ecology and Evolution*, 3, 217–223.

Ronellenfitsch, H., Liesche, J., Jensen, K.H., Holbrook, N.M., Schulz, A. & Katifori, E. (2015) Scaling of phloem structure and optimality of photoassimilate transport in conifer needles. *Proceedings of the Royal Society B: Biological Sciences*, 282, 20141863.

Russell, S.H. & Evert, R.F. (1985) Leaf vasculature in *Zea mays* L. *Planta*, 164, 448–458.

Sack, L. & Scoffoni, C. (2013) Leaf venation: structure, function, development, evolution, ecology and applications in the past, present and future. *New Phytologist*, 198, 983–1000.

Sack, L., Scoffoni, C., John, G.P., Poorter, H., Mason, C.M., Mendez-Alonzo, R. et al. (2013) How do leaf veins influence the worldwide leaf economic spectrum? review and synthesis. *Journal of Experimental Botany*, 64, 4053–4080.

Sack, L., Scoffoni, C., McKown, A.D., Frole, K., Rawls, M., Havran, J.C. et al. (2012) Developmentally based scaling of leaf venation architecture explains global ecological patterns. *Nature Communications*, 3, 837.

Sage, R.F. (2004) The evolution of C_4 photosynthesis. *New Phytologist*, 161, 341–370.

Salvi, A.M., Smith, D.D., Adams, M.A., McCulloh, K.A. & Givnish, T.J. (2021) Mesophyll photosynthetic sensitivity to leaf water potential in eucalyptus: a new dimension of plant adaptation to native moisture supply. *New Phytologist*, 230, 1844–1855.

Shi, P., Liu, M., Ratkowsky, D.A., Gielis, J., Su, J., Yu, X. et al. (2019) Leaf area-length allometry and its implications in leaf shape evolution. *Trees*, 33, 1073–1085.

Skinner, R. (1994) Epidermal cell division and the coordination of leaf and tiller development. *Annals of Botany*, 74, 9–15.

Smith, D.D. & Sperry, J.S. (2014) Coordination between water transport capacity, biomass growth, metabolic scaling and species stature in co-occurring shrub and tree species. *Plant, Cell & Environment*, 37, 2679–2690.

Sperry, J.S., Hacke, U.G. & Wheeler, J.K. (2005) Comparative analysis of end wall resistivity in xylem conduits. *Plant, Cell & Environment*, 28, 456–465.

Stickler, F.C., Wearden, S. & Pauli, A.W. (1961) Leaf area determination in grain Sorghum[1]. *Agronomy Journal*, 53, 187–188.

Taylor, S.H., Hulme, S.P., Rees, M., Ripley, B.S., Ian Woodward, F. & Osborne, C.P. (2010) Ecophysiological traits in C_3 and C_4 grasses: a phylogenetically controlled screening experiment. *New Phytologist*, 185, 780–791.

Volkenburgh, E.V. (1999) Leaf expansion—an integrating plant behaviour. *Plant, Cell & Environment*, 22, 1463–1473.

Warton, D.I., Wright, I.J., Falster, D.S. & Westoby, M. (2006) Bivariate line-fitting methods for allometry. *Biological Reviews*, 81, 259–291.

Watcharamongkol, T., Christin, P.-A. & Osborne, C.P. (2018) C_4 photosynthesis evolved in warm climates but promoted migration to cooler ones. *Ecology Letters*, 21, 376–383.

Wilson, D. & Cooper, J.P. (1967) Assimilation of *Lolium* in relation to leaf mesophyll. *Nature*, 214, 989–992.

Wright, I.J., Reich, P.B., Westoby, M., Ackerly, D.D., Baruch, Z., Bongers, F. et al. (2004) The worldwide leaf economics spectrum. *Nature*, 428, 821–827.

Zhong, M., Cerabolini, B.E.L., Castro-Díez, P., Puyravaud, J.-P. & Cornelissen, J.H.C. (2020) Allometric co-variation of xylem and stomata across diverse woody seedlings. *Plant, Cell & Environment*, 43, 2301–2310.

SUPPORTING INFORMATION

Additional supporting information can be found online in the Supporting Information section at the end of this article.

How to cite this article: Baird, A.S., Taylor, S.H., Reddi, S., Pasquet-Kok, J., Vuong, C., Zhang, Y. et al. (2024) Allometries of cell and tissue anatomy and photosynthetic rate across leaves of C_3 and C_4 grasses. *Plant, Cell & Environment*, 47, 156–173. https://doi.org/10.1111/pce.14741